ACS OMEGA

http://pubs.acs.org/journal/acsodf

Article

One-Pot Extraction and Quantification Method for Bile Acids in the Rat Liver by Capillary Liquid Chromatography Tandem Mass Spectrometry

Tomomi Asano, Kentaro Taki, Kazuya Kitamori, Hisao Naito, Tamie Nakajima, Hitoshi Tsuchihashi, Akira Ishii, and Kei Zaitsu*

Cite This: *ACS Omega* 2021, 6, 8588−8597

Read Online

ACCESS | Metrics & More | Article Recommendations | Supporting Information

ABSTRACT: We developed a highly sensitive method for quantifying 21 bile acids (BAs) in the rat liver by capillary liquid chromatography tandem mass spectrometry (cLC/MS/MS) with one-pot extraction. High recovery rates were obtained for the one-pot methods with either methanol (MeOH) extraction or MeOH/acetonitrile (ACN) (1:1, v/v) mixture extraction; the results obtained for the MeOH/ACN mixture solution were better than the results obtained for MeOH. Thus, we determined that the one-pot method with MeOH/ACN was the most suitable method for the efficient extraction of BAs in the liver. Targeted BAs were well separated by cLC with gradient elution using ammonium acetate (NH_4OAc)−MeOH mobile phases. Method validation proved that the intra-day and inter-day accuracies and precisions were primarily less than ±20 and 20% relative standard deviation, respectively. Also, the limit of detection (LOD) and the limit of quantitation (LOQ) were 0.9−10 and 2.3−27 ng/g liver, which proves the high sensitivity of the method. Finally, we quantitated 21 BA concentrations in the liver samples of normal and nonalcoholic steatohepatitis (NASH) rats, both of which were derived from stroke-prone spontaneously hypertensive five (SHRSP5) /Dmcr rat. The hepatic BA profiles were found to be substantially different between the normal and NASH groups; the two groups were clearly separated along the first component axis in the score plots of the principal component analysis. In particular, 10 BAs (β-muricholic acid (MCA), glyco (G-) cholic acid (CA), G-chenodeoxycholic acid (CDCA), tauro (T-) CA, T-CDCA, T-ursodeoxycholic acid (UDCA), T-lithocholic acid (LCA), T-hiodeoxycholic acid (HDCA), T-α-MCA, and T-β-MCA) were significantly different between the two groups using Welch's *t*-test with the false discovery rate correction method, demonstrating BA disruption in the NASH model rat. In conclusion, this method was able to quantify 21 BAs in the rat liver and will evaluate the hepatic BA pathophysiology of rat disease models.

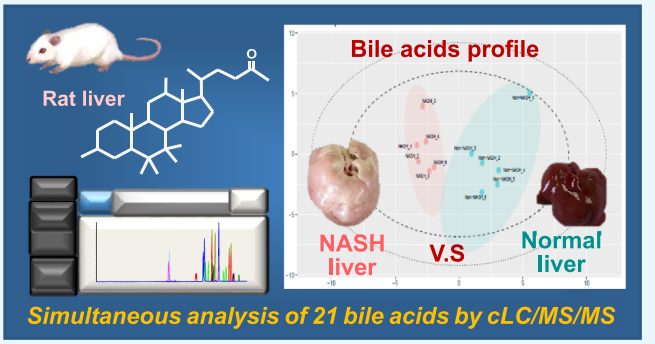

INTRODUCTION

Bile acids (BAs) have numerous isomers; different forms for primary and secondary BAs and conjugates are generated during biosynthesis and metabolism. BAs have recently been used as biomarkers for various diseases, such as obesity and type 2 diabetes,[1] because of their role as signal molecules in regulating biosynthesis and energy homeostasis.[2,3] In addition, Josef et al. reported that BAs have potential as biomarkers for diagnosing Alzheimer's disease.[4]

Each BA plays an important role in the digestion and absorption of lipid nutrition,[5] although some BAs show cytotoxicity because of their detergency.[6] Thus, abnormal changes in the composition and accumulation of BAs, especially in the liver, can be a risk factor for various diseases. In particular, their accumulation in the hepatocyte is strongly related to chronic liver diseases such as liver fibrosis, cirrhosis, and cancer.[7,8] Our previous study[9] using nonalcoholic steatohepatitis (NASH) model rats[10] demonstrated that the expressions of cytochrome P450 7A1 (CYP 7A1) (cholesterol-7-α-hydroxylase) and CYP 7B1 (oxysterol-7-α-hydroxylase), which are involved in BA homeostasis, were upregulated. In addition, the expressions of CYP 8B1 (sterol-12-α-hydroxylase), CYP 27A1 (sterol-27-α-hydroxylase), and bile salt export pump, which are involved in BA excretion, were downregulated. These results strongly suggested that changes in the BA composition were related to the development of NASH. Based on these results, we need to understand the more detailed hepatic profile of BAs in the NASH pathology.

Received: January 22, 2021
Accepted: March 5, 2021
Published: March 16, 2021

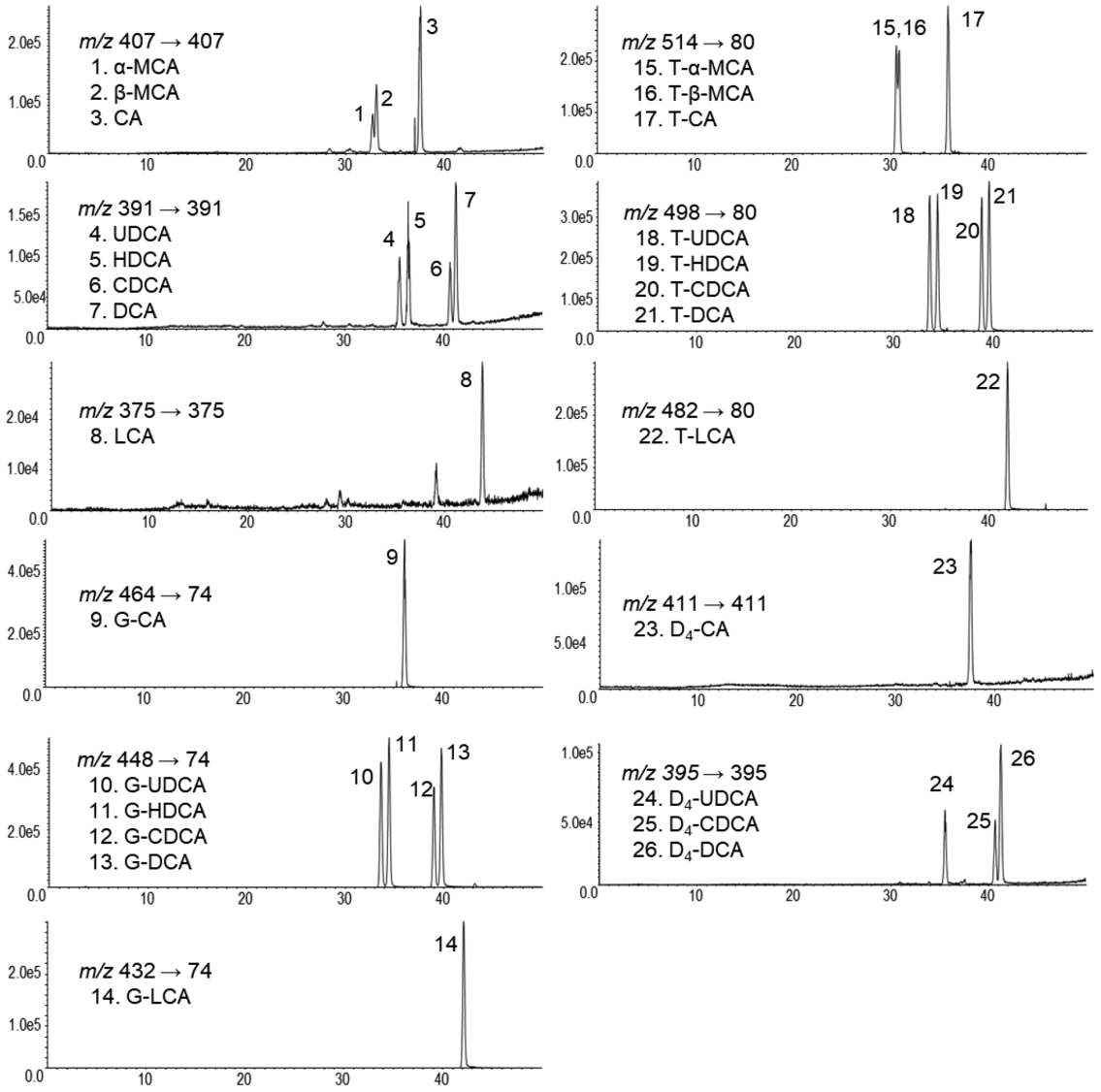

Figure 1. SRM chromatograms of BA standards (50 ng/mL) obtained by cLC/MS/MS

As described above, it is necessary to discriminate the isomers of BAs because numerous such isomers exist in nature. Currently, gas chromatography mass spectrometry (GC/MS)[11−13] and liquid chromatography tandem mass spectrometry (LC/MS/MS)[14−20] are being widely used in the analysis of BAs. LC/MS/MS is useful in detecting and quantifying BAs in tissue samples because it does not require the derivatization of target compounds. To improve MS identification, LC/high-resolution MS (HRMS) has been applied to the analysis of BAs.[21−23] However, improvements in LC separation are needed to separate BA isomers, which can potentially be achieved by LC with narrow inner diameters, such as capillary LC (cLC) and nano-LC. The cLC method is more practical than the nano-LC method because the flow rate and back pressure can be easily controlled. Chervet et al. stated that cLC needs to be applied with a flow rate of 1−10 μL/min and an inner separation column diameter of 150−500 μm.[24] The cLC-based methods have been used in various fields in which the sensitivity and separation of the targets are superior to those of the targets used in the conventional methods.[25−31] However, there has been only one report on the application of cLC for analyzing BAs in urine,[32] and there have been no reports on the use of cLC/MS/MS for analyzing BAs in the rat liver.

In this study, we developed a cLC/MS/MS-based method for the analysis of BAs in the rat liver. We optimized an extraction method of BAs in the rat liver and validated the quantitativity of the method. Finally, our method was applied to normal and NASH rats, and the usefulness of this approach was evaluated.

RESULTS AND DISCUSSION

Optimization of cLC/MS/MS. The MS parameters for each BA were optimized using the enhanced product ion (EPI) scan mode (collision energy: -130− to 5 eV) by infusion analysis. The optimized selected reaction monitoring (SRM) transitions and collision energies (CEs) are described in the Materials and Methods section (Table 3). The free BAs were not easily dissociated, and no characteristic product ions except for the deprotonated ions ($[M-H]^-$) were observed for the free BAs. Thus, the precursor ions (i.e., the deprotonated ions) were passed through Q3 and detected as the product ions. As shown in Table 3, chenodeoxycholic acid (CDCA), deoxycholic acid (DCA), ursodeoxycholic acid (UDCA), and

https://dx.doi.org/10.1021/acsomega.1c00403
ACS Omega 2021, 6, 8588−8597

Table 1. Linearity, LOD, LOQ, Matrix Effect, Recovery, and Intra-Day and Inter-Day Repeatability

								intra-day				inter-day			
								QC sample1[c] (100 ng/g liver)		QC sample2[c] (750 ng/g liver)		QC sample1[c] (100 ng/g liver)		QC sample2[c] (750 ng/g liver)	
bile acid (BA)	internal standard	range	linearity	LOD[a]	LOQ[a]	matrix effect[b]	recovery[b]	accuracy	precision	accuracy	precision	accuracy	precision	accuracy	precision
		(ng/g liver)	(r^2)	(ng/g liver)		(%)	(%)	(%)	(% RSD)	(%)	(% RSD)	(%)	(% RSD)	(%)	(% RSD)
CA	D_4-CA	2.5−1000	0.998	1.8	5.2	74.8 ± 5.1	80.4 ± 8.4	104	1.8	95.4	0.4	101	5.1	97.7	3.2
CDCA	D_4-CDCA	2.5−1000	0.999	1.3	3.5	71.3 ± 2.5	71.9 ± 7.2	104	5.2	97.8	4.8	97.2	3.6	100	6.9
DCA	D_4-DCA	2.5−1000	0.999	1.5	4.4	74.2 ± 3.6	72.0 ± 3.1	98.7	3.4	96.2	1.1	99.0	4.4	96.6	2.3
UDCA	D_4-UDCA	2.5−1000	0.999	1.5	4.1	78.1 ± 6.3	83.7 ± 5.0	100	2.5	101	2.7	100	2.1	96.7	0.9
HDCA	D_4-CA	2.5−1000	0.998	5.1	16	66.1 ± 1.7	83.4 ± 7.4	102	1.5	84.0	12	99.5	3.4	84.1	2.6
α-MCA	D_4-CA	2.5−1000	0.951	1.8	4.3	109 ± 13	103 ± 22	94.9	9.8	107	9.6	106	9.1	130	15
β-MCA	D_4-CA	2.5−1000	0.994	0.9	2.3	87.2 ± 16	112 ± 27	103	4.0	103	6.4	108	9.0	113	8.9
G-CA	D_4-CA	2.5−1000	0.994	7.9	23	86.8 ± 1.5	93.5 ± 13	105	2.6	93.0	6.7	105	4.4	114	2.5
G-CDCA	D_4-CA	2.5−1000	0.998	3.5	10	90.3 ± 4.7	88.5 ± 12	101	0.8	105	3.6	99.1	6.4	109	1.8
G-DCA	D_4-CA	2.5−1000	0.996	6.8	19	94.2 ± 2.3	86.4 ± 10	101	1.4	102	6.7	102	5.2	110	1.5
G-UDCA	D_4-CA	2.5−1000	0.990	9.1	25	93.0 ± 3.4	88.1 ± 4.2	106	4.2	107	4.4	99.2	3.9	115	16
G-LCA	D_4-CA	2.5−1000	0.995	3.6	11	99.1 ± 1.6	76.1 ± 9.8	85.2	4.0	105	6.9	88.9	11	94.2	5.8
G-HDCA	D_4-CA	2.5−1000	0.992	10	27	95.1 ± 7.7	90.3 ± 5.1	104	3.9	103	5.5	103	4.3	117	4.7
T-CA	D_4-CA	2.5−1000	0.994	4.9	15	87.4 ± 6.0	86.1 ± 6.0	103	2.6	97.9	6.7	110	6.7	111	12
T-CDCA	D_4-CA	2.5−1000	0.996	4.4	13	87.7 ± 2.8	82.6 ± 9.5	99.7	2.3	105	4.8	103	8.3	113	3.9
T-DCA	D_4-CA	2.5−1000	0.997	4.2	12	85.4 ± 2.7	86.2 ± 9.8	99.1	0.8	104	7.5	101	8.1	110	8.1
T-UDCA	D_4-CA	2.5−1000	0.992	5.9	16	94.7 ± 2.9	85.6 ± 3.9	102	4.6	111	3.2	105	7.3	119	13
T-LCA	D_4-CA	2.5−1000	0.995	2.9	9.3	87.4 ± 2.1	75.7 ± 9.5	83.7	4.7	108	6.8	90.1	11	94.2	5.9
T-HDCA	D_4-CA	2.5−1000	0.994	5.4	15	96.9 ± 4.3	83.3 ± 4.3	101	2.6	106	5.5	107	4.2	118	11
T-α-MCA	D_4-CA	2.5−1000	0.996	2.7	7.3	85.3 ± 1.9	93.9 ± 6.7	103	2.1	108	3.6	116	7.2	118	11
T-β-MCA	D_4-CA	2.5−1000	0.997	1.9	5.7	87.8 ± 2.8	96.2 ± 8.0	98.7	4.5	107	3.9	113	4.4	118	11

[a]Concentration of extract solution. [b]Evaluated at 50 ng/mL solution. [c]n = 4 each.

https://dx.doi.org/10.1021/acsomega.1c00403
ACS Omega 2021, 6, 8588−8597

hiodeoxycholic acid (HDCA) are isomers; their glycine and taurine conjugates also have the same molecular weight. Moreover, they exhibit identical optimized SRM transitions. Thus, these isomers must be separated by chromatography. In this study, we compared ammonium acetate (NH_4OAc)−methanol (MeOH)-based and NH_4OAc−acetonitrile (ACN)-based mobile phases. When the NH_4OAc−ACN-based mobile phase was used, UDCA and HDCA were not sufficiently separated (Figure S1-a). Although the peaks of CDCA and DCA were partially separated, their spectra overlapped. In addition, the glycine and taurine conjugates of UDCA and HDCA were coeluted (Figures S1-b and S1-c). However, their peaks were well separated when the NH_4OAc−MeOH-based mobile phase was used (Figure S2). Therefore, we selected the NH_4OAc−MeOH-based mobile phase for LC separation. These compounds were well separated because of their strong retention in the column, which resulted from the high polarity of the NH_4OAc−MeOH-based mobile phase. Furthermore, NH_4OAc can suppress peak tailing and improve peak shapes,[19] which contribute to successful separation.

Although good separation of BAs was achieved using the NH_4OAc−MeOH-based mobile phase, a 90 min duration was required to separate all the target BAs. Therefore, we further improved the LC gradient conditions. We increased the gradient curve during the initial part of the gradient condition (see the Materials and Methods section), which decreased the total analysis time (57 min). The chromatograms obtained under the optimized conditions are shown in Figure 1.

Extraction of BAs in Rat Liver Samples. Although effective procedures for BA extraction have been reported by other researchers,[15,17,18] these approaches require two steps: (1) homogenization with a mixture of distilled water and MeOH and (2) deproteinization and desalting with alkaline ACN. In this study, we additionally performed a one-step extraction method—homogenization and deproteinization were performed in one pot. Here, we compared three solvents: (1) MeOH, (2) ACN, and (3) the MeOH/ACN (1:1, v/v) mixture solution.

We applied the two-step extraction method with water/MeOH and the one-pot methods with different solvents to wild-type rat (Wister Kyoto, WKY) liver samples; the relative recovery rates are shown in Figure S3. High recovery rates were obtained using the one-pot methods by either MeOH extraction or MeOH/ACN mixture extraction; the MeOH/ACN mixture solution showed better results than MeOH. Furthermore, because of the deproteinization effect of ACN,[33] the extract obtained using the one-pot method with MeOH/ACN was a more visually translucent sample solution than that obtained using the one-pot method with MeOH. Thus, we determined that the one-pot method with MeOH/ACN was the most suitable for efficient extraction.

Method Validation. In general, calibration curves are prepared with spiked samples. However, BAs endogenously exist in liver samples; therefore, blank extracts are required for method validation.[14,15,17,18,20] Other researchers have reported using activated charcoal for preparing blank extracts, and the amount of added activated charcoal differed depending on the use: 0.2−0.5 mg/mg for liver samples,[15,18] 50−100 mg/mL for serum samples,[14,15,18] and 3 mg/mg for brain samples.[20] In our study, we initially treated the liver samples with activated charcoal at 0.5 mg/mg; however, some BAs were not fully removed. Therefore, we prepared blank liver extracts by the duplicate treatment of activated charcoal at 0.5 mg/mg, as a result of which no BA was detected in the extract (Table S1).

The validation results for the proposed method are listed in Table 1. In our pre-experiments, LCA was not detected in the liver samples of the normal and NASH groups (Figure S4) (as described in more detail later). Therefore, method validation for LCA was not performed. The calibration curves show good linearity (correlation coefficient (r^2) = 0.990−0.999) except for α-muricholic acid (MCA) (r^2 = 0.951) in the range of 2.5−1000 ng/g liver. The limit of detection (LOD) and the limit of quantitation (LOQ) values were 0.9−10 ng/g liver and 2.3−27 ng/g liver, respectively. Also, the precision values (%RSD) near the lower end of the calibration range (5 ng/g liver) were under 14% RSD (Table S2). This cLC/MS/MS method enables a highly sensitive analysis of BAs despite using a low injection volume (2 μL).

The matrix effects exceeded 80% for most of the BAs, although the values for free BAs were slightly lower (ca. 70%) except for α-MCA and β-MCA (109 and 87.2%). This is mainly due to their lower ionization efficiencies because there are no polar moieties in their chemical structures. The recovery rates exceeded 80%, except for CDCA and DCA (ca. 70%), and G-LCA and T-LCA (ca. 76%). In this study, the MeOH/ACN mixture was used for extraction; thus, the recovery rates of low-polar BAs such as CDCA and DCA tended to be somewhat low. As shown in Figure 1, LCA was strongly retained (retention time: ca. 43 min), suggesting that the hydrophobicity of LCA was significantly strong. Also, the retention times of G-LCA and T-LCA were the same as that of LCA; that is, these conjugates were strongly hydrophobic. Thus, the recovery rates of G-LCA and T-LCA became somewhat lower than those of other conjugates. The intra-day and inter-day accuracies were 83.7−106% and 88.9−116% for the quality control (QC) sample 1 (corresponding to 100 ng/g liver) and 84.0−111% and 84.1−130% for QC sample 2 (corresponding to 750 ng/g liver). The intra-day and inter-day precisions were 0.8−9.8% relative standard deviation (RSD) and 2.1−11% RSD for QC sample 1 and 0.4−12% RSD and 0.9−16% RSD for QC sample 2. The intra-day and inter-day accuracies and precisions were below 20%, excluding the accuracy of α-MCA for QC sample 2 (30%); these results prove the validity of our method.

Profiling of Hepatic BAs in Normal and NASH Rats. NASH is a type of nonalcoholic fatty liver disease and is characterized by progression from a simple fatty liver to chronic inflammation, fibrosis, cirrhosis, and hepatocellular carcinoma. Kitamori et al. developed a NASH model rat[10] based on a stroke-prone spontaneously hypertensive five (SHRSP5)/Dmcr rat with an eight-week intake of high-fat and cholesterol (HFC) diet, as shown in Table S3. Jia et al. demonstrated that the NASH model rat exhibited expression changes in BA synthetase and excretion transporters.[9] Moreover, this model rat developed fibrotic steatohepatitis, which resulted in changes in the BA profile of the liver.[34] In this study, we applied the cLC/MS/MS method to the normal (not fibrotic steatohepatitis) and NASH rats to evaluate the effectiveness and validity of our method.

The quantitative results for the BAs are shown in Table 2. Although LCA was successfully detected in the liver of WKY rats (wild type rats), it was not detected in either the normal or NASH rats. These results matched well with the results of our previous report.[34] Other studies have also reported that the concentration of LCA in a rodent's liver was undetectable or

https://dx.doi.org/10.1021/acsomega.1c00403
ACS Omega 2021, 6, 8588−8597

Table 2. Quantitative BA Results for Liver Samples from SHRSP5/Dmcr Rat[a]

BA	normal group (ng/g liver) average ± SD	NASH group (ng/g liver) average ± SD	VIP value	q value
CA	119 ± 149	32 ± 16	0.73	N.A.
CDCA	90 ± 63	93 ± 35	0.40	N.A.
DCA	44 ± 29	44 ± 36	0.04	N.A.
UDCA	357 ± 211	130 ± 74	0.97	N.A.
HDCA	345 ± 241	158 ± 71	0.78	N.A.
α-MCA	658 ± 382	547 ± 113	0.45	N.A.
β-MCA	71 ± 24	24 ± 13	1.09	0.0151
G-CA	701 ± 693	2699 ± 634	1.38	0.0020
G-CDCA	106 ± 104	1129 ± 486	1.32	0.0044
G-DCA	313 ± 348	864 ± 676	0.77	N.A.
G-UDCA	371 ± 520	156 ± 68	0.58	N.A.
G-LCA	23 ± 26	42 ± 26	0.64	N.A.
G-HDCA	66 ± 61	76 ± 77	0.24	N.A.
T-CA	3331 ± 1189	802 ± 299	1.32	0.0044
T-CDCA	942 ± 243	731 ± 304	0.62	N.A.
T-DCA	1694 ± 424	460 ± 311	1.36	0.0020
T-UDCA	1873 ± 620	62 ± 24	1.42	0.0027
T-LCA	282 ± 119	49 ± 30	1.28	0.0052
T-HDCA	941 ± 340	34 ± 42	1.38	0.0034
T-α-MCA	1302 ± 337	590 ± 249	1.23	0.0044
T-β-MCA	2138 ± 438	1131 ± 605	1.12	0.0105

[a]N.A., not applicable.

very low.[15,18,35,36] Moreover, the other 21 BAs were successfully detected in the liver of the normal and NASH rats. The quantitative results for the normal and NASH groups were confirmed as reliable because there was no difference in their matrix effects, as shown in Table S4. The principal component analysis (PCA) score and loading plots for these data are shown in Figure 2. In the PCA score plots, the normal and NASH groups were well separated, which demonstrated that their BA profiles were substantially different. The PCA loading plots show that glycocholic acid (G-CA), glycochenodeoxycholic acid (G-CDCA), and taurine-conjugated BAs are primarily responsible for group separation. Furthermore, projection to latent structures−discriminant analysis (PLS−DA) was performed (Figure S5), and variable importance in projection (VIP) and q values were calculated (Table 2). Finally, the levels of 10 BAs were significantly different between the normal and NASH groups (significance level at 0.05); their box-and-whisker plots are shown in Figure 3. Among these BAs, the levels of G-CA and G-CDCA were significantly higher in the NASH group, and the other BAs showed significantly lower levels. This method enabled the simultaneous analysis of BAs in the rat liver with a low sample injection volume. In particular, the high-precision analysis of low-concentration BAs enabled us to identify subtle changes in the liver samples of the normal and NASH groups.

CONCLUSIONS

In this study, we developed a reliable cLC/MS/MS-based quantitative method for 21 BAs in the rat liver. We optimized various one-pot extraction methods using different solvents and determined that MeOH/ACN was the most suitable for the efficient extraction of BAs in the liver. The targeted BAs were well separated by cLC with gradient elution using the NH_4OAc-MeOH mobile phases. The method validation showed satisfactory results: the intra- and inter-day accuracies and precisions were primarily less than ±20 and 20% RSD, which proved the high quantitativity of the method. Also, the LOD and LOQ values were 0.9−10 ng/g and 2.3−27 ng/g liver, respectively, which proved the high sensitivity of the method. Finally, we applied the method to normal and NASH rats. The two groups were clearly separated in the PCA score plots; the PCA loading plots suggested that G-CA, G-CDCA, and taurine conjugates strongly contributed to group separation in the PCA score plots. In particular, significant differences were found for 10 BAs between the two groups; these values revealed the differences in the BA profiles between the normal and NASH groups. This method will help elucidate the hidden pathophysiological properties of BAs in various disease models.

MATERIALS AND METHODS

Materials and Reagents. The BA standards used in this study are listed in Table 3. We used eight unconjugated BAs, six glycine-conjugated BAs, and eight taurine-conjugated BAs. These BAs were obtained from FUJIFILM Wako Pure Chemical Corporation (Osaka, Japan), Merck (Darmstadt, Germany), Santa Cruz Biotechnology (Santa Cruz, California, USA), Sigma-Aldrich (St. Louis, MI), and Steraloids (Newport, RI). Four deuterium-labeled (D_4) BAs were purchased from CDN Isotopes Inc. (Pointe-Claire, Quebec, Canada) for use as internal standards (ISs). MeOH, ACN, distilled water, and NH_4OAc were of the LC−MS grade, obtained from Sigma-Aldrich (St. Louis, MI) and Kanto Chemical (Tokyo, Japan).

Animals. WKY rats (wild-type rats) were distributed by the Disease Model Cooperative Research Association (Kyoto, Japan). The rats were housed in plastic cages for 5 days after their arrival and were given ad libitum access to SP diet (Funabashi Farm, Chiba, Japan), as a normal diet for SHRSP strain rats, and water. The rearing room was controlled on a 12-h light−dark cycle (lights off at 9:00 pm), and the room temperature was maintained at 25 ± 1 °C.

The normal and NASH rats were prepared from the SHRSP5/Dmcr rats (Disease Model Cooperative Research Association, Kyoto, Japan), which were differentiated from the WKY rats in accordance with our previous report.[10] The NASH model rats were prepared from 10-week male SHRSP5/Dmcr rats with the HFC diet for 8 weeks. The normal (not fibrotic steatohepatitis) rats were prepared from 18-week SHRSP5/Dmcr rats with SP diets. The nutrient components of the SP and HFC diets are listed in Table S3. All the animal experiments were approved by the Experimental Animal Research Committee of Kinjo Gakuin University (Authorization number 10).

cLC/MS/MS Conditions. Instrumental analysis was performed using a DiNa-2A nano-LC (KYA Tech, Tokyo, Japan) coupled with a 4000 Q-TRAP mass spectrometer (Sciex, Framingham, MA, USA). LC separation was performed using an L-column2 ODS (300 μm i.d. × 50 mm, 3 μm particle size; Chemicals Evaluation and Research Institute, Tokyo, Japan). The mobile phases were as follows: A (10% MeOH in 10 mM NH_4OAc aqueous solution); B (98% MeOH in 10 mM NH_4OAc aqueous solution). The gradient conditions were as follows: 0−5 min: 0−25% B; 5−42 min: 25−100% B; 42−47 min: 100% B; 47−47.1 min: 100−0% B; 47.1−57 min:

https://dx.doi.org/10.1021/acsomega.1c00403
ACS Omega 2021, 6, 8588−8597

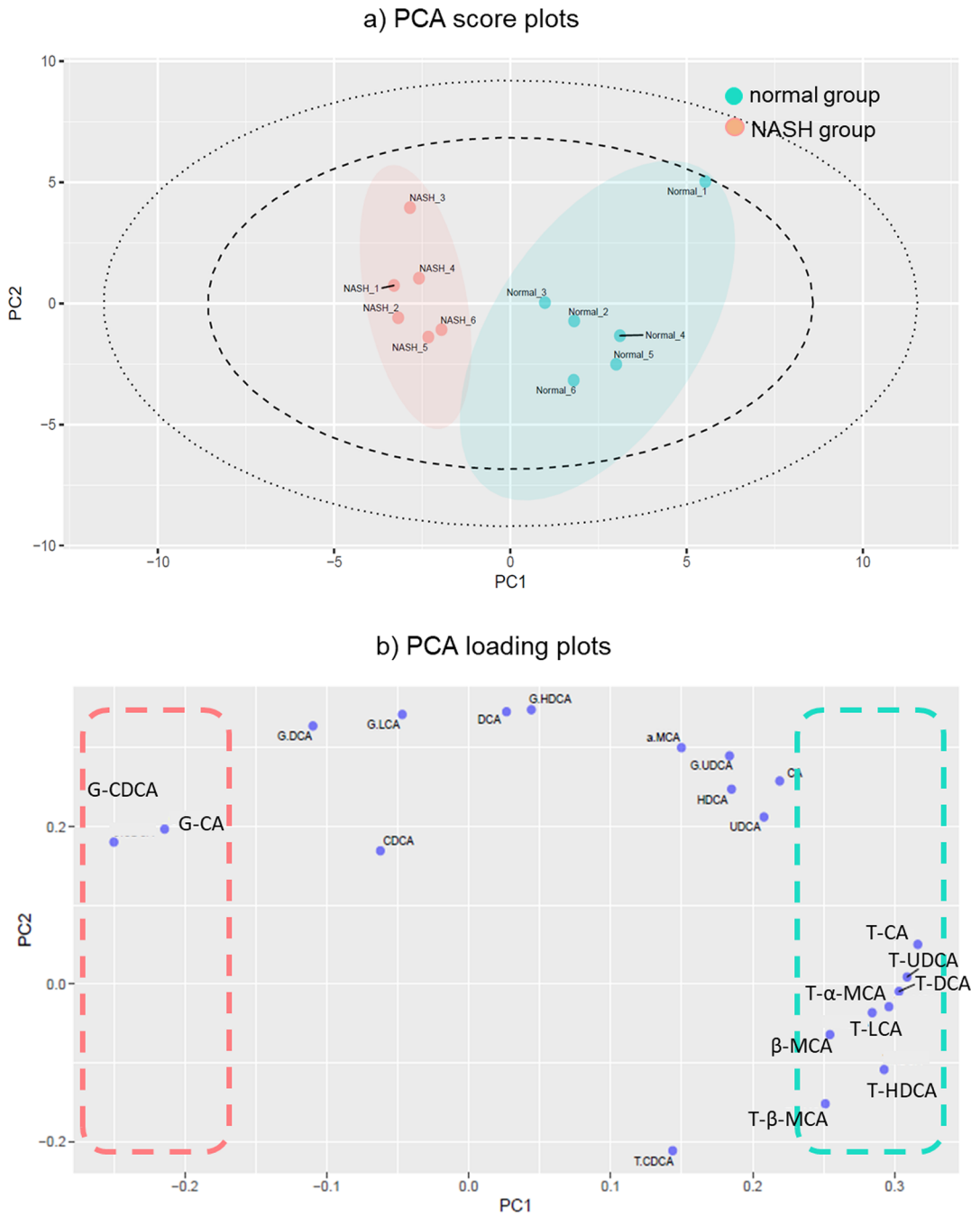

Figure 2. PCA for the normal and NASH groups: (a) PCA score plots; (b) PCA loading plots.

0% B. The total flow rate was 1 μL/min, and the injection volume was 2 μL.

The measurements were performed in the ESI-negative mode. The remaining MS parameters were as follows: curtain gas at 10 AU; collision gas at 6 AU; ion spray voltage of -1300 V; interface heater temperature of 150 °C; declustering potential of −20 V; entrance potential of −10 V; and collision cell exit potential of −15 V. The analytes were monitored in the SRM mode using the SRM transitions and CEs shown in Table 3.

Preparation of Blank Liver Extract. The blank liver extract was prepared by removing endogenous BAs from 18-week-old WKY rat liver. The liver extracts were homogenized with a five-fold volume of the MeOH and ACN mixture (1:1, v/v) using a multisample organ homogenizer (Multi-beads shocker, Yasui Kikai, Osaka, Japan) rotated at the speed of 2500 rpm for 40 s. Then, the liver homogenate was centrifuged at 13,000 g for 10 min. Activated charcoal was added to the supernatant at 0.1 mg/μL (corresponding to 0.5 mg/mg liver), and the samples were vortexed for 30 min at room temperature. After centrifugation, the supernatant was placed in a new Eppendorf tube. Additional activated charcoal (0.1 mg/μL) was added to the sample, which was then vortexed for 30 min. After centrifugation, the obtained supernatant was used as a blank liver extract.

Calibration Curves and Method Validation. BA-standard MeOH solutions were prepared at 1 mg/mL each and stored at 4 °C. BA working mixture solutions were prepared at

https://dx.doi.org/10.1021/acsomega.1c00403
ACS Omega 2021, 6, 8588−8597

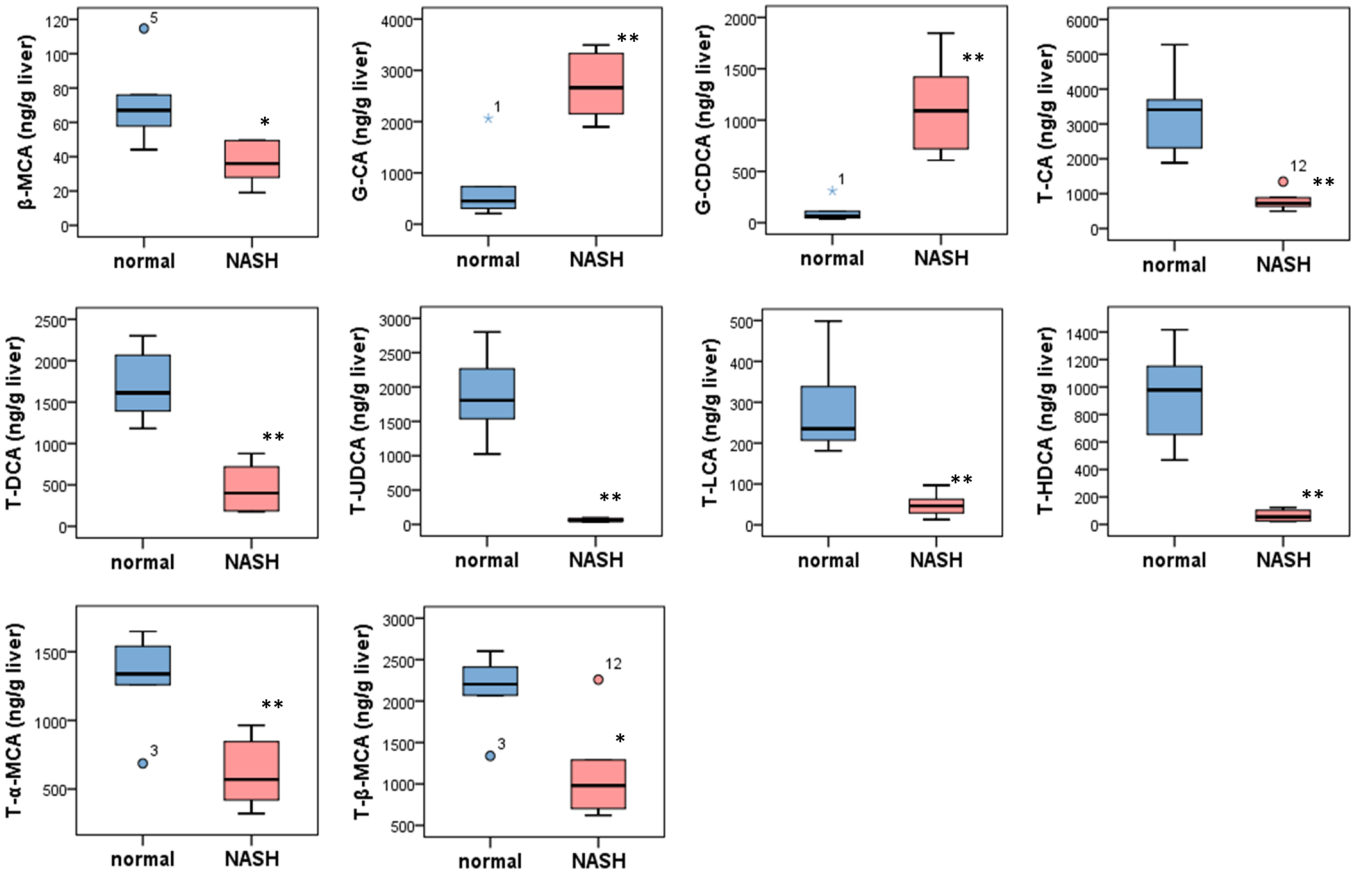

Figure 3. Box-and-whisker plots of the BAs exhibiting significant changes (*q < 0.05, **q < 0.01).

Table 3. BAs and Their SRM Transitions and CEs

	compound name	SRM transition	collision energy (eV)
free-BA	cholic acid (CA)	407 → 407	−15
	chenodeoxycholic acid (CDCA)	391 → 391	−30
	deoxycholic acid (DCA)	391 → 391	−30
	ursodeoxycholic acid (UDCA)	391 → 391	−30
	lithocholic acid (LCA)	375 → 375	−30
	hiodeoxycholic acid (HDCA)	391 → 391	−30
	α-murichoric acid (α-MCA)	407 → 407	−15
	β-muricholic acid (β-MCA)	407 → 407	−15
glyco-BA	glycocholic acid (G-CA)	464 → 74	−70
	glycochenodeoxycholic acid (G-CDCA)	448 → 74	−70
	glycodeoxycholic acid (G-DCA)	448 → 74	−70
	glycoursodeoxycholic acid (G-UDCA)	448 → 74	−70
	glycolithocholic acid (G-LCA)	432 → 74	−70
	glycohiodeoxycholic acid (G-HDCA)	448 → 74	−70
tauro-BA	taurocholic acid (T-CA)	514 → 80	−125
	taurochenodeoxycholic acid (T-CDCA)	498 → 80	−125
	taurodeoxycholic acid (T-DCA)	498 → 80	−125
	tauroursodeoxycholic acid (T-UDCA)	498 → 80	−125
	taurolithocholic acid (T-LCA)	482 → 80	−125
	taurohiodeoxycholic acid (T-HDCA)	498 → 80	−125
	tauro-α-murichoric acid (T-α-MCA)	514 → 80	−125
	tauro-β-muricholic acid (T-β-MCA)	514 → 80	−125
internal standard	D_4-cholic acid (D_4-CA)	411 → 411	−15
	D_4-chenodeoxycholic acid (D_4-CDCA)	395 → 395	−30
	D_4-ceoxycholic acid (D_4-DCA)	395 → 395	−30
	D_4-ursodeoxycholic acid (D_4-UDCA)	395 → 395	−30

https://dx.doi.org/10.1021/acsomega.1c00403
ACS Omega 2021, 6, 8588−8597

2.5, 25, 50, 250, 500, and 1000 ng/mL prior to the experiments, and an IS mixture solution in MeOH was adjusted to 250 ng/mL. Calibration curves were constructed using six calibrants (2.5, 25, 50, 250, 500, and 1000 ng/g liver, n = 4 for each calibrant sample), which were produced by spiking the working mixture solutions in blank liver extracts. To prepare calibrants, 10 μL of the working mixture solution of each concentration and 10 μL of IS were added to 50 μL of the blank liver extract. Then, the sample was evaporated using a centrifugal concentrator at room temperature. The residue was reconstituted with 50 μL of 10% MeOH in 10 mM NH_4OAc and filtrated through a 0.22 μm filter.

The theoretical LOD and LOQ were determined by analyzing the calibrants and calculated according to the formula: LOD = 3sd/a, LOQ = 10sd/a (sd = the standard deviation of y = intercepts of regression lines and a = slope of the calibration curve).[37] The recovery rates were calculated by comparing the results between the pre-spiked and post-spiked samples using blank liver extracts. The matrix effects were calculated by comparing the results between the post-spiked sample and a standard mixture solution (50 ng/mL each). Method validation was performed using two QC samples (QC sample 1 with 100 ng/g liver and QC sample 2 with 750 ng/g liver), and the intra-day and inter-day accuracies and precisions were evaluated.

Preparation of Rat Liver Samples. Approximately 20 mg of the liver sample was homogenized in a five-fold volume of the MeOH/ACN (1:1, v/v) mixture solution with respect to the liver weight, and the homogenate was centrifuged at 13,000 g for 10 min. After 10 μL of the IS mixture solution (250 ng/mL each) was spiked in 50 μL of the supernatant, the sample was evaporated using a centrifugal concentrator at room temperature for 1 h. The residue was reconstituted in 50 μL of 10% MeOH in 10 mM NH_4OAc and filtrated through a 0.22 μm filter.

Statistical Analysis. The differences in the BA profiles between the normal and NASH groups were evaluated by the PCA using the R software version 3.6.3.[38] The R script was demonstrated in our previous study.[39] PLS−DA was further applied to the results, and the VIP values were calculated. In our previous reports,[39,40] the VIP value-based approach was applied to determine the statistical family. Here, the BAs with VIP values over 1.0 were selected as a statistical family. The statistical differences of BAs were evaluated using Welch's t-test, where the p levels were adjusted to control multiple comparisons using the FDR procedure proposed by Benjamini and Hochberg,[41] and the adjusted values were expressed as q values (significance level at 0.05).

■ ETHICAL GUIDELINES

We performed animal experiments in accordance with the Regulations on Animal Experiments at Kinjo Gakuin University and in accordance with the Fundamental Guidelines for the Proper Conduct of Animal Experiment and Related Activities at Academic Research Institutions (Notice No. 71 of the Ministry of Education, Culture, Sports, Science, and Technology in Japan, 2006).

■ ASSOCIATED CONTENT

Supporting Information

The Supporting Information is available free of charge at https://pubs.acs.org/doi/10.1021/acsomega.1c00403.

BA residual rates after the activated charcoal treatment; the precision near the lower end of the calibration range; nutrient components of the SP and HFC diets; comparison of matrix effects in WKY and SHRSP 5/Dmcr rats in the liver; SRM chromatograms of UDCA, HDCA, CDCA, and DCA standards obtained using the NH_4OAc−ACN-based mobile phase; SRM chromatograms of UDCA, HDCA, CDCA, and DCA standards obtained using the NH_4OAc−MeOH-based mobile phase; comparison of BAs detected in WKY rat liver samples using the four extraction methods; SRM chromatograms of LCA in the SHRSP5/Dmcr rat liver; and PLS−DA for the normal and NASH groups (PDF)

■ AUTHOR INFORMATION

Corresponding Author

Kei Zaitsu − *Department of Legal Medicine & Bioethics, Nagoya University Graduate School of Medicine, Nagoya 466-8550, Japan; In Vivo Real-time Omics Laboratory, Institute for Advanced Research, Nagoya University, Nagoya 464-8601, Japan*; Phone: +81-52-755-2118; Email: kzaitsu@med.nagoya-u.ac.jp; Fax: +81−52- 744-2121

Authors

Tomomi Asano − *Department of Human Life and Environment, Kinjo Gakuin University, Nagoya 463-8521, Japan; Department of Legal Medicine & Bioethics, Nagoya University Graduate School of Medicine, Nagoya 466-8550, Japan*; orcid.org/0000-0002-1095-396X

Kentaro Taki − *Department of Legal Medicine & Bioethics, Nagoya University Graduate School of Medicine, Nagoya 466-8550, Japan*

Kazuya Kitamori − *Department of Human Life and Environment, Kinjo Gakuin University, Nagoya 463-8521, Japan*

Hisao Naito − *Department of Human Life and Environment, Kinjo Gakuin University, Nagoya 463-8521, Japan*

Tamie Nakajima − *College of Life and Health Sciences, Chubu University, Kasugai, Aichi 487-8501, Japan*

Hitoshi Tsuchihashi − *Department of Legal Medicine & Bioethics, Nagoya University Graduate School of Medicine, Nagoya 466-8550, Japan*

Akira Ishii − *Department of Legal Medicine & Bioethics, Nagoya University Graduate School of Medicine, Nagoya 466-8550, Japan*

Complete contact information is available at: https://pubs.acs.org/10.1021/acsomega.1c00403

Author Contributions

K.Z. conceived the idea, designed the experiment, and supervised the experiments. K.Z. and T.A. wrote the manuscript. T.A. performed the experiments, and K.T. assisted in instrumental analysis. T.A., K.K., and H.N. conducted the animal experiments. K.Z. and T.A. discussed the results, and T.N. and A.I. commented on the manuscript.

Notes

The authors declare no competing financial interest.

https://dx.doi.org/10.1021/acsomega.1c00403
ACS Omega 2021, 6, 8588−8597

■ ACKNOWLEDGMENTS

This study was partially supported by JSPS KAKENHI Grant Number 19 K11653. We would like to thank the anonymous reviewers who strongly improved the manuscript with their feedback and comments.

■ REFERENCES

(1) Lei, S.; Huang, F.; Zhao, A.; Chen, T.; Chen, W.; Xie, G.; Zheng, X.; Zhang, Y.; Yu, H.; Zhang, P.; Rajani, C.; Bao, Y.; Jia, W.; Jia, W. The ratio of dihomo-gamma-linolenic acid to deoxycholic acid species is a potential biomarker for the metabolic abnormalities in obesity. *Faseb J.* **2017**, *31*, 3904−3912.

(2) Keitel, V.; Kubitz, R.; Häussinger, D. Endocrine and paracrine role of bile acids. *World J. Gastroenterol.* **2008**, *14*, 5620−5629.

(3) Thomas, C.; Pellicciari, R.; Pruzanski, M.; Auwerx, J.; Schoonjans, K. Targeting bile-acid signalling for metabolic diseases. *Nat. Rev. Drug Discov.* **2008**, *7*, 678−693.

(4) Marksteiner, J.; Blasko, I.; Kemmler, G.; Koal, T.; Humpel, C. Bile acid quantification of 20 plasma metabolites identifies lithocholic acid as a putative biomarker in Alzheimer's disease. *Metabolomics* **2018**, *14*, 1.

(5) Tso, P. Gastrointestinal digestion and absorption of lipid. *Adv. Lipid Res.* **1985**, *21*, 143−186.

(6) Cai, X.; Grant, D. J. W.; Wiedmann, T. S. Analysis of the solubilization of steroids by bile salt micelles. *J. Pharm. Sci.* **1997**, *86*, 372−377.

(7) Hofmann, A. F. The continuing importance of bile acids in liver and intestinal disease. *Arch. Intern. Med.* **1999**, *159*, 2647−2658.

(8) Monte, M. J.; Marin, J. J.; Antelo, A.; Vazquez-Tato, J. Bile acids: chemistry, physiology, and pathophysiology. *World J. Gastroenterol.* **2009**, *15*, 804−816.

(9) Jia, X.; Naito, H.; Yetti, H.; Tamada, H.; Kitamori, K.; Hayashi, Y.; Wang, D.; Yanagiba, Y.; Wang, J.; Ikeda, K.; Yamori, Y.; Nakajima, T. Dysregulated bile acid synthesis, metabolism and excretion in a high fat-cholesterol diet-induced fibrotic steatohepatitis in rats. *Dig. Dis. Sci.* **2013**, *58*, 2212−2222.

(10) Kitamori, K.; Naito, H.; Tamada, H.; Kobayashi, M.; Miyazawa, D.; Yasui, Y.; Sonoda, K.; Tsuchikura, S.; Yasui, N.; Ikeda, K.; Moriya, T.; Yamori, Y.; Nakajima, T. Development of novel rat model for high-fat and high-cholesterol diet-induced steatohepatitis and severe fibrosis progression in SHRSP5/Dmcr. *Environ. Health Prev. Med.* **2012**, *17*, 173−182.

(11) Griffiths, W. J.; Sjövall, J. Bile acids: analysis in biological fluids and tissues. *J. Lipid Res.* **2010**, *51*, 23−41.

(12) Kumar, B. S.; Chung, B. C.; Lee, Y. J.; Yi, H. J.; Lee, B. H.; Jung, B. H. Gas chromatography-mass spectrometry-based simultaneous quantitative analytical method for urinary oxysterols and bile acids in rats. *Anal. Biochem.* **2011**, *408*, 242−252.

(13) Tadano, T.; Kanoh, M.; Matsumoto, M.; Sakamoto, K.; Kamano, T. Studies of serum and feces bile acids determination by gas chromatography-mass spectrometry. *Rinsho Byori.* **2006**, *54*, 103−110.

(14) Ando, M.; Kaneko, T.; Watanabe, R.; Kikuchi, S.; Goto, T.; Iida, T.; Hishinuma, T.; Mano, N.; Goto, J. High sensitive analysis of rat serum bile acids by liquid chromatography/electrospray ionization tandem mass spectrometry. *J. Pharm. Biomed. Anal.* **2006**, *40*, 1179−1186.

(15) Alnouti, Y.; Csanaky, I. L.; Klaassen, C. D. Quantitative-profiling of bile acids and their conjugates in mouse liver, bile, plasma, and urine using LC-MS/MS. *J. Chromatogr., B* **2008**, *873*, 209−217.

(16) Scherer, M.; Gnewuch, C.; Schmitz, G.; Liebisch, G. Rapid quantification of bile acids and their conjugates in serum by liquid chromatography-tandem mass spectrometry. *J. Chromatogr., B* **2009**, *877*, 3920−3925.

(17) Huang, J.; Bathena, S. P. R.; Csanaky, I. L.; Alnouti, Y. Simultaneous characterization of bile acids and their sulfate metabolites in mouse liver, plasma, bile, and urine using LC-MS/MS. *J. Pharm. Biomed. Anal.* **2011**, *55*, 1111−1119.

(18) Suzuki, Y.; Kaneko, R.; Nomura, M.; Naito, H.; Kitamori, K.; Nakajima, T.; Ogawa, T.; Hattori, H.; Seno, H.; Ishii, A. Simple and rapid quantitation of 21 bile acids in rat serum and liver by UPLC-MS-MS: effect of high fat diet on glycine conjugates of rat bile acids. *Nagoya J. Med. Sci.* **2013**, *75*, 57−71.

(19) Li, K.; Buchinger, T. J.; Bussy, U.; Fissette, S. D.; Johnson, N. S.; Li, W. Quantification of 15 bile acids in lake charr feces by ultra-high performance liquid chromatography-tandem mass spectrometry. *J. Chromatogr., B* **2015**, *1001*, 27−34.

(20) Higashi, T.; Watanabe, S.; Tomaru, K.; Yamazaki, W.; Yoshizawa, K.; Ogawa, S.; Nagao, H.; Minato, K.; Maekawa, M.; Mano, N. Unconjugated bile acids in rat brain: Analytical method based on LC/ESI-MS/MS with chemical derivatization and estimation of their origin by comparison to serum levels. *Steroids* **2017**, *125*, 107−113.

(21) Amplatz, B.; Zöhrer, E.; Haas, C.; Schäffer, M.; Stojakovic, T.; Jahnel, J.; Fauler, G. Bile acid preparation and comprehensive analysis by high performance liquid chromatography-high-resolution mass spectrometry. *Clin. Chim. Acta* **2017**, *464*, 85−92.

(22) Lee, G.; Lee, H.; Hong, J.; Lee, S. H.; Jung, B. H. Quantitative profiling of bile acids in rat bile using ultrahigh-performance liquid chromatography-orbitrap mass spectrometry: Alteration of the bile acid composition with aging. *J. Chromatogr., B* **2016**, *1031*, 37−49.

(23) Minato, K.; Suzuki, M.; Nagao, H.; Suzuki, R.; Ochiai, H. Development of analytical method for simultaneous determination of five rodent unique bile acids in rat plasma using ultra-performance liquid chromatography coupled with time-of-flight mass spectrometry. *J. Chromatogr., B* **2015**, *1002*, 399−410.

(24) Chervet, J. P.; Ursem, M.; Salzmann, J. P. Instrumental requirements for nanoscale liquid chromatography. *Anal. Chem.* **1996**, *68*, 1507−1512.

(25) Wu, Y. R.; Liu, H. Y.; Lin, S. L.; Fuh, M. R. Quantification of 7-aminoflunitrazepam in human urine by polymeric monolith-based capillary liquid chromatography coupled to tandem mass spectrometry. *Talanta* **2018**, *176*, 293−298.

(26) Wilson, R. E.; Jaquins-Gerstl, A.; Weber, S. G. On-Column Dimethylation with Capillary Liquid Chromatography-Tandem Mass Spectrometry for Online Determination of Neuropeptides in Rat Brain Microdialysate. *Anal. Chem.* **2018**, *90*, 4561−4568.

(27) Yuan, W.; Zhang, J.; Li, S.; Edwards, J. L. Amine metabolomics of hyperglycemic endothelial cells using capillary LC-MS with isobaric tagging. *J. Proteome Res.* **2011**, *10*, 5242−5250.

(28) Ding, J.; Sorensen, C. M.; Zhang, Q.; Jiang, H.; Jaitly, N.; Livesay, E. A.; Shen, Y.; Smith, R. D.; Metz, T. O. Capillary LC coupled with high-mass measurement accuracy mass spectrometry for metabolic profiling. *Anal. Chem.* **2007**, *79*, 6081−6093.

(29) Wang, J.; Zhang, Y.; Jiang, H.; Cai, Y.; Qian, X. Phosphopeptide detection using automated online IMAC-capillary LC-ESI-MS/MS. *Proteomics* **2006**, *6*, 404−411.

(30) Liu, X.; Lovell, M. A.; Lynn, B. C. Development of a method for quantification of acrolein-deoxyguanosine adducts in DNA using isotope dilution-capillary LC/MS/MS and its application to human brain tissue. *Anal. Chem.* **2005**, *77*, 5982−5989.

(31) Shen, Y.; Tolić, N.; Zhao, R.; Pasa-Tolić, L.; Li, L.; Berger, S. J.; Harkewicz, R.; Anderson, G. A.; Belov, M. E.; Smith, R. D. High-throughput proteomics using high-efficiency multiple-capillary liquid chromatography with on-line high-performance ESI FTICR mass spectrometry. *Anal. Chem.* **2001**, *73*, 3011−3021.

(32) Yang, Y.; Griffiths, W. J.; Nazer, H.; Sjovall, J. Analysis of bile acids and bile alcohols in urine by capillary column liquid chromatography-mass spectrometry using fast atom bombardment or electrospray ionization and collision-induced dissociation. *Biomed. Chromatogr.* **1997**, *11*, 240−255.

(33) Jones, D. R.; Wu, Z.; Chauhan, D.; Anderson, K. C.; Peng, J. A nano ultra-performance liquid chromatography-high resolution mass spectrometry approach for global metabolomic profiling and case study on drug-resistant multiple myeloma. *Anal. Chem.* **2014**, *86*, 3667−3675.

https://dx.doi.org/10.1021/acsomega.1c00403
ACS Omega 2021, 6, 8588−8597

(34) Jia, X.; Suzuki, Y.; Naito, H.; Yetti, H.; Kitamori, K.; Hayashi, Y.; Kaneko, R.; Nomura, M.; Yamori, Y.; Zaitsu, K.; Kato, M.; Ishii, A.; Nakajima, T. A possible role of chenodeoxycholic acid and glycine-conjugated bile acids in fibrotic steatohepatitis in a dietary rat model. *Dig. Dis. Sci.* **2014**, *59*, 1490−1501.
(35) Yang, T.; Shu, T.; Liu, G.; Mei, H.; Zhu, X.; Huang, X.; Zhang, L.; Jiang, Z. Quantitative profiling of 19 bile acids in rat plasma, liver, bile and different intestinal section contents to investigate bile acid homeostasis and the application of temporal variation of endogenous bile acids. *J. Steroid Biochem. Mol. Biol.* **2017**, *172*, 69−78.
(36) García-Cañaveras, J. C.; Donato, M. T.; Castell, J. V.; Lahoz, A. Targeted profiling of circulating and hepatic bile acids in human, mouse, and rat using a UPLC-MRM-MS-validated method. *J. Lipid Res.* **2012**, *53*, 2231−2241.
(37) Currie, L. A. Limits for qualitative detection and quantitative determination. Application to radiochemistry. *Anal. Chem.* **1968**, *40*, 586−593.
(38) R Core Team *R: A Language and Environment for Statistical Computing*, R Foundation for Statiscal Computing: Vienna, Austria, 2020.
(39) Zaitsu, K.; Eguchi, S.; Ohara, T.; Kondo, K.; Ishii, A.; Tsuchihashi, H.; Kawamata, T.; Iguchi, A. PiTMaP: A New Analytical Platform for High-Throughput Direct Metabolome Analysis by Probe Electrospray Ionization/Tandem Mass Spectrometry Using an R Software-Based Data Pipeline. *Anal. Chem.* **2020**, *92*, 8514−8522.
(40) Zaitsu, K.; Noda, S.; Iguchi, A.; Hayashi, Y.; Ohara, T.; Kimura, Y.; Koketsu, Y.; Kosaki, T.; Kusano, M.; Sato, T.; Ishikawa, T.; Tsuchihashi, H.; Suzuki, K.; Ishii, A. Metabolome analysis of the serotonin syndrome rat model: Abnormal muscular contraction is related to metabolic alterations and hyper-thermogenesis. *Life Sci.* **2018**, *207*, 550−561.
(41) Benjamini, Y.; Hochberg, Y. Controlling the False Discovery Rate: A Practical and Powereful Approach to Multiple Testing. *J. Royal Statis. Soc. Statis. Methodol. Ser. B* **1995**, *57*, 289−300.

https://dx.doi.org/10.1021/acsomega.1c00403
ACS Omega 2021, 6, 8588−8597